OUT-OF-PLANE SEISMIC PERFORMANCE OF PLASTERBOARD PARTITION WALLS VIA QUASI-STATIC TESTS

Petrone C.[1], Magliulo G.[*1], Lopez P.[2], Manfredi G.[1]

[1]*Department of Structures for Engineering and Architecture, University of Naples Federico II, Naples, Italy*

[2]*Technical Development Center, Siniat, 500 Rue Marcel Demonque, 84915 Avignon, France*

ABSTRACT

Internal partitions, as many nonstructural components, should be subjected to a careful and rational seismic design, as for structural elements. A quasi-static test campaign aimed at the evaluation of the out-of-plane seismic performance of Siniat plasterboard internal partitions with steel studs is conducted according to FEMA 461 testing protocol. Four tall, i.e. 5 m high, specimens are selected from the range of internal partition developed in Europe by Siniat, a leading supplier of plasterboard components in Europe.

Under the specified testing protocol, a significant nonlinear pinched behavior of the tested specimen is observed. The pinched behavior is caused by the damage in the screwed connections, whose cyclic behavior is strongly degrading. Both stiffness and strength of the specimens are significantly influenced by the board typology and the amount of screwed connections. Finally, it is concluded that Eurocodes significantly underestimate the resisting bending moment of the tested specimens.

KEYWORDS

Nonstructural components, internal partitions, quasi-static test, seismic performance, cold-formed steel stud.

---

[*] Correspondence to: Prof. Gennaro Magliulo, Department of Structures for Engineering and Architecture, via Claudio 21, 80125 Naples, Italy. E-mail gmagliul@unina.it. tel +390817683464. fax +390817685921

1 INTRODUCTION

The seismic performance of nonstructural components is nowadays recognized to be a key issue in the framework of the Performance-Based Earthquake Engineering (PBEE). Indeed, PBEE explicitly defines different accepted damage levels for non-structural components and contents at different levels of seismic excitations (Bertero and Bertero 2002), according to a multi-level seismic design approach. Four main issues motivate research studies on this topic.

- Nonstructural components generally exhibit damage for low seismic demand levels. The seismic performance of nonstructural components is crucial in frequent, and less intense, earthquakes, where their damage can cause the inoperability of several buildings. For instance, damage in partition walls and infill walls caused the evacuation, and the consequent downtime, of several lightly damaged reinforced concrete structures after 2009 L'Aquila earthquake.
- The cost of nonstructural components represents the largest portion of the building construction cost. Indeed, Taghavi and Miranda (2003) showed that structural cost only corresponds to 18%, 13% and 8% of the construction cost for offices, hotels and hospitals respectively.
- The failure of nonstructural components can also cause injuries or deaths; the threatening to the life safety due to nonstructural components increases if it is considered that suffocation is the most common cause of death due to an earthquake. The 64% of the fatalities caused by 1995 Great Hanshin Earthquake was due to the suffocation of the human body due to compression or obstruction (Ikuta and Miyano 2011). Such a phenomenon could be caused by the damage to nonstructural components, which may limit the accessibility of an egress route.
- Nonstructural components may participate in the lateral system of the primary structure at often unknown levels, i.e. varying the lateral strength and stiffness of the structural system. However, the behavior in the out-of-plane direction of internal partitions, which is the focus of this paper, gives a negligible contribution to the global behavior of the primary structure.

The following research study deals with "tall", i.e. 5 m high, plasterboard internal partitions for industrial and commercial buildings. Plasterboard internal partitions with steel stud are classified as architectural nonstructural components according to Villaverde (1997). They, as many nonstructural components, should be subjected to a careful and rational seismic design, as for the structural elements, given the above mentioned motivations.

Several research studies on the seismic assessment of plasterboard internal partitions characterized by cold-formed steel studs can be found in the literature, e.g. (Lee et al. 2007; Restrepo and Lang 2011; Restrepo and Bersofsky 2011; Tasligedik et al. 2012; Magliulo et al. 2012). Fifty tests on cold-formed steel stud internal partitions were conducted at the University at Buffalo as part of the NEES Nonstructural Grand Challenge project. Thirty-six internal partition walls were tested in-plane under quasi-static (Retamales et al. 2013) and dynamic loading protocols, whereas fourteen wall specimens were dynamically tested in the out-of-plane direction (Davies et al. 2011) by means of the University at Buffalo Nonstructural Component Simulator (UB-NCS). The influence given by the presence of a bookshelf and/or return walls on the global behavior of the specimen is investigated. However, the tested components do not reflect the typical partitions used in European countries, being representative of US construction market.

Bidirectional shake table tests on innovative drywall internal partitions are described in Magliulo et al. (2014). This test campaign aims at the evaluation of the seismic performance of an innovative partition system considering in-plane and out-of-plane interaction. A steel test frame is designed in order to simulate the seismic effects at a generic building story. The AC 156 (International Conference of Building Officials (ICBO) 2000) testing protocol is adopted.

According to current building codes, e.g. Eurocode 8 (CEN 2004b), partition systems are nonstructural components, which must be designed in order to withstand a predefined seismic action. Their seismic design is performed by comparing the seismic demand on the component with the capacity of the partition system. The assessment is performed in the out-of-plane direction since internal partitions are acceleration-sensitive components in such a direction. While the seismic demand can be assessed by means of code formulae, the seismic capacity should be evaluated through either experimental tests or reliable analytical/numerical models. Dynamic tests should be preferred in the assessment of the capacity through experimental tests. However, in this study quasi-static tests were considered, as detailed in the following Sections.

In the available literature there is very limited evidence of out-of-plane quasi-static tests on plasterboard partitions, aimed at the evaluation of their seismic performance in terms of strength, stiffness and ductility. However, some similar studies are available concerning structural walls made by steel studs (Peterman and Schafer 2014), which significantly differ from the internal partitions both in terms of applied loads and in terms of components. Moreover, tests in the out-of-plane direction are typically performed by private companies according to ASTM E-72 standard (ASTM 2015), but they are not publicly accessible.

In this research study, quasi-static tests are performed on 5 m tall plasterboard internal partitions built with Siniat products, aiming at evaluating their seismic performance in terms of strength, stiffness and ductility. This partition typology is commercialized in Europe by Siniat, a leading supplier of plasterboard components, for industrial and commercial buildings. A test setup is designed in order to perform quasi-static tests on such components. Four different specimens, from Siniat partition offer, are subjected to the quasi-static test protocol provided by FEMA 461 (FEMA 461 2007). The typical damage typologies are shown as well as the recorded force-displacement envelopes. Finally, a critical comparison with the current European building code is discussed.

2 EXPERIMENTAL FACILITIES, TEST SETUP, SPECIMENS AND TEST PROTOCOL

A quasi-static test campaign is conducted in the Laboratory of the Technical Development Center of Siniat International Company in Avignon, France (Figure 1 and Figure 2). The tests are aimed at assessing the out-of-plane seismic behavior of internal plasterboard partitions installed in industrial and commercial buildings, which are typically characterized by large interstory height.

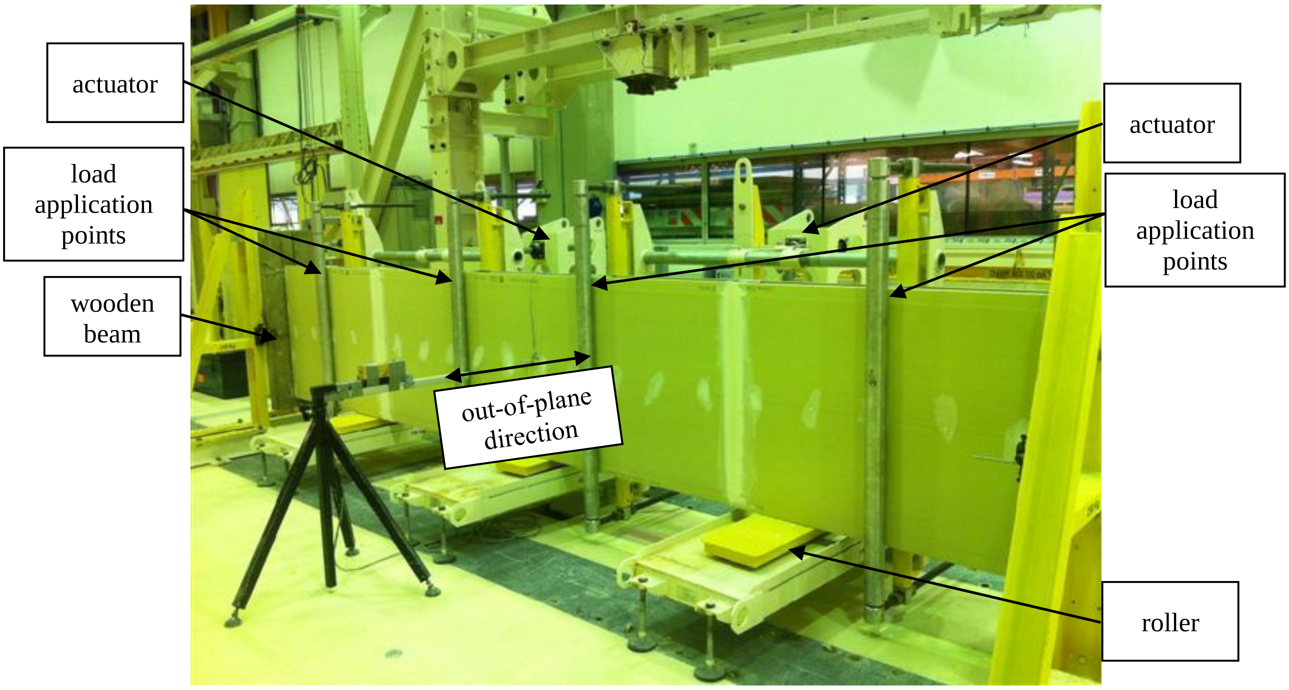

Figure 1. Global view of the test setup for specimen no. 1.

Figure 2. Details of the actuator and the load application points (specimen no. 2).

The specimens are representative of Siniat plasterboard partitions with steel studs. In particular, four different 5 m high plasterboard partitions are tested. Their selection, performed by an industrial partner committee, reflects the typical high partition configurations for industrial buildings that are commercialized by Siniat in European countries. They are also selected since in-plane quasi-static tests were performed on these specimens, as detailed in Petrone et al. (2015a). Quasi-static tests were preferred to dynamic tests since the available facilities did not allow to dynamically investigate the tall partitions considered in this study.

2.1 Test setup

A single vertical "strip" of each partition is tested in this test campaign, characterized by the width of a single vertical plasterboard. It is implicitly assumed that the partition is wide enough in order to neglect the contribution of the adjacent boards in the horizontal direction. The specimen is placed horizontally (Figure 1) in order to accommodate the features of the available facility. The test is based on the six point bending scheme shown in Figure 3. The test setup provides two actuators placed symmetrically with respect to the center of the specimen; each actuator is characterized by two application points (Figure 2). The total force applied to the partition is therefore divided into four different forces, which are characterized by the same magnitude. The four forces are positioned in order to reproduce a bending moment diagram similar to the one that would occur for a uniformly distributed load acting in the out-of-plane direction.
The external restraints are given by two wooden beams, which are fixed at the base by steel elements. These beams are made of wood in order to facilitate the installation of the steel guides.

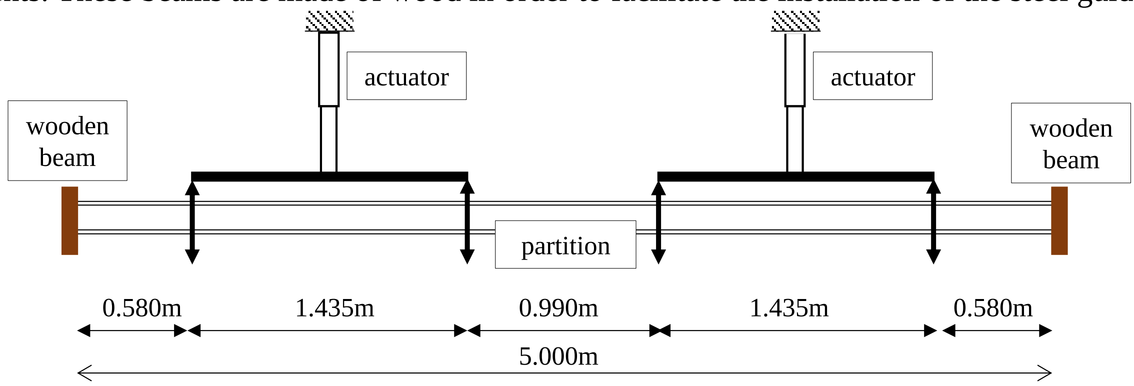

Figure 3. Top view on the specimen: six point bending scheme adopted for the test campaign.

2.2 Specimens

Specimen no. 1 is 5000 mm high and 900 mm wide. Its cross-section is depicted in Figure 4a; it is composed of the following components:

- two horizontal (vertical in the test setup) Siniat U-shaped guides made of 0.6 mm thick galvanized steel; they are screwed into wooden beams (Figure 1) which are positioned at the top and at the base of the partition;
- a single vertical (horizontal in the test setup) Siniat C-shaped stud made of 0.6 mm thick galvanized steel; it is called M100-50, because it is characterized by 50 mm wide flanges and by a 100 mm wide web;
- a 18 mm thick Siniat plasterboard layer on each side of the partition. The plasterboards are connected both to the stud and to the horizontal guides by 250 mm spaced screws; even though all types of boards are 2600 mm high, three boards are adjacently installed in order to reach the 5000 mm height according to the construction practice (Figure 1). The horizontal joints are sealed with paper and Siniat joint compound.

Specimen no. 1 is representative of a partition with 900 mm spaced studs. Specimen no. 2 is characterized by two layers of 1200 mm wide and 12.5 mm thick plasterboards for each side (Figure 4b). The plasterboards are screwed to two M150-50 studs, which are 600 mm spaced; inner plasterboards are connected to the studs with a 600 mm spaced screwed connections, whereas the outer plasterboards are characterized by 300 mm spacing. Specimen no. 3 is characterized by two layers of 1200 mm wide and 12.5 mm thick plasterboards for each side, which are screwed to two back-to-back M150-50 studs with a 600 mm spacing (Figure 4c). Specimen no. 4 is characterized by two layers of 1200 mm wide and 18 mm thick plasterboards for each side, screwed to three back-to-back studs M100-50 with a 400 mm spacing (Figure 4d); inner plasterboards are connected to the stud with a 600 mm spaced screwed connections, whereas the outer plasterboards are characterized by 300 mm spacing. The main features of the tested specimens are summarized in Table 1.

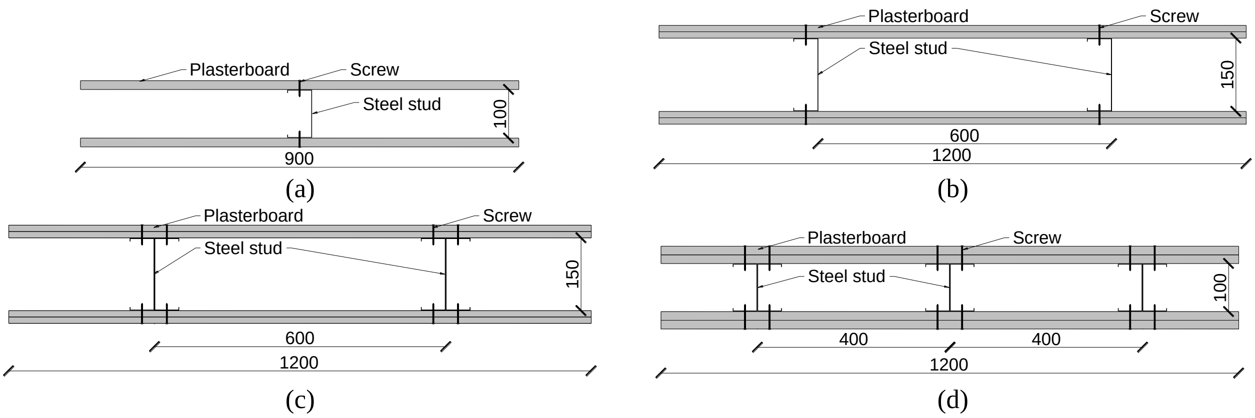

Figure 4. Test specimen cross-sections: (a) specimens no. 1, (b) specimen no. 2, (c) specimen no. 3 and (d) specimen no. 4.

Specimen no.	Siniat stud	Siniat plasterboard	Siniat guide
1	50-100-50 mm section with 6 mm lips, 0.6 mm thick, 900 mm spacing	1 layer of BA18S boards 18 mm thick, 900 mm wide	30-100-30mm “U” section, 0.6mm thick
2	50-150-50 mm section with 6 mm lips, 0.6 mm thick, 600 mm spacing	2 layers of BA13 boards 12.5 mm thick, 1200 mm wide	50-150-50mm “U” section, 0.6mm thick
3	50-150-50 mm section with 6 mm lips, back to back, 0.6 mm thick, 600 mm spacing	2 layers of BA13 boards 12.5 mm thick, 1200 mm wide	50-150-50mm “U” section, 0.6mm thick
4	50-100-50 mm section with 6 mm lips, back to back, 0.6mm thick, 400 mm spacing	2 layers of BA18 boards 18 mm thick, 1200 mm wide	30-100-30mm “U” section, 0.6mm thick

Table 1. Components adopted for the different specimens.

Steel studs are characterized by 300 N/mm^2 tensile strength and 210000 N/mm^2 elastic modulus resulting from tensile tests on stud specimens. BA13 board is characterized by a 3.31 N/mm^2 compressive strength and 1.84 N/mm^2 tensile strength; BA18 board exhibits a 5.50 N/mm^2 compressive strength and 1.57 N/mm^2 tensile strength, whereas BA18S board exhibits a 8.16 N/mm^2 compressive strength and a 1.43 N/mm^2 tensile strength. The elastic modulus range is 2410-5240 N/mm^2. The self-drilling screws adopted for the different specimens are characterized by a 3.5 mm diameter, 35 mm length and a flat head. Finally, a global picture of the four tested specimens is reported in Figure 5.

Specimen no. 1

Specimen no. 2

Specimen no. 3

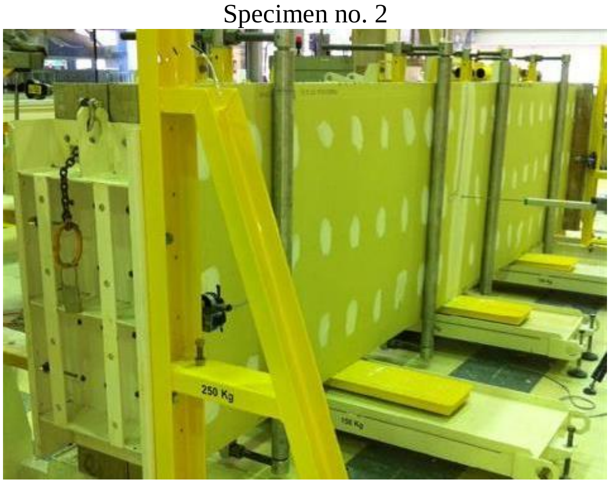

Specimen no. 4

Figure 5. Global view on the four tested specimens.

2.3 Test protocol

The protocol of the quasi-static test is defined according to FEMA 461 “Interim Testing Protocols for Determining the Seismic Performance Characteristics of Structural and Nonstructural

Components” (FEMA 461 2007). FEMA 461 proposes the loading history as a numeric succession of two consecutive steps with amplitude a_i and a_{i+1}, respectively, according to the following relationship:

$$a_{i+1} = c \cdot a_i \tag{1}$$

Two cycles at the same displacement amplitude a_i are provided for each step. Equation (1) is calibrated in order to be representative of the response of SDOF systems subjected to a set of ground motions in ordinary conditions recorded in the US region. The suggested value of the parameter c is 1.4.

Based on the research study included in Petrone et al. (2015a), which is based on earthquakes recorded in Europe, the parameter c is slightly modified in 1.39. A 100 mm target displacement Δ_m at the 15th step of the loading protocol is defined, which is representative of the collapse displacement of the partition. In case the collapse of the partitions is not exhibited at the target displacement value, the loading history is continued by using further increments of amplitude of 0.3 times Δ_m, i.e. 30 mm, according to FEMA 461. The displacement loading protocol is depicted in Figure 6, assuming a total number of steps equal to 20.

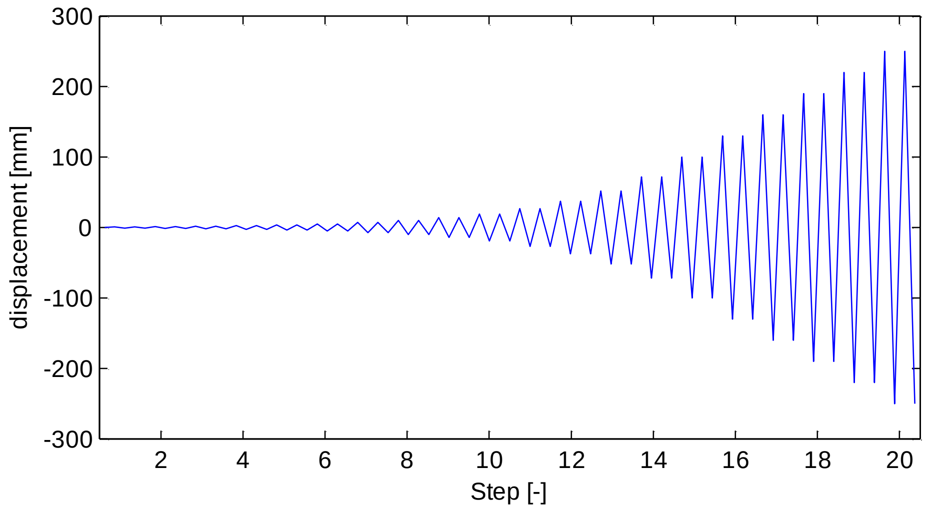

Figure 6. Adopted displacement loading protocol.

2.4 Instrumentation

Several instruments are selected in order to monitor the response of the specimens when subjected to the predefined loading protocol. A Linear Variable Displacement Transducer (LVDT) is placed at the centroid of the partition in order to record the mid-span out-of-plane displacement of the partition (Figure 7a). Several strain gauges are placed at different points of the specimen:

- four strain gauges are placed on the inner and on the external faces of the boards at the centroid of the partition, i.e. strain gauges A, B, C and D in Figure 7b;
- three strain gauges are positioned on three different cross-sections of a steel stud, according to the arrangement provided in Figure 7b, i.e. strain gauges E, F and G. The three selected cross-sections are corresponding to: (a) the force application point closest to the external support, (b) the centroid of the partition and (c) the horizontal joint between the plasterboard panels.

Two LVDTs are also installed in order to monitor relative displacements in the out-of-plane direction between the external wooden beam and the partition, both at the base and at the top of the partition. Finally, two LVDTs are installed to measure the absolute displacement of the external wooden beams in the out-of-plane direction, in order to verify the effectiveness of their restraining effect.

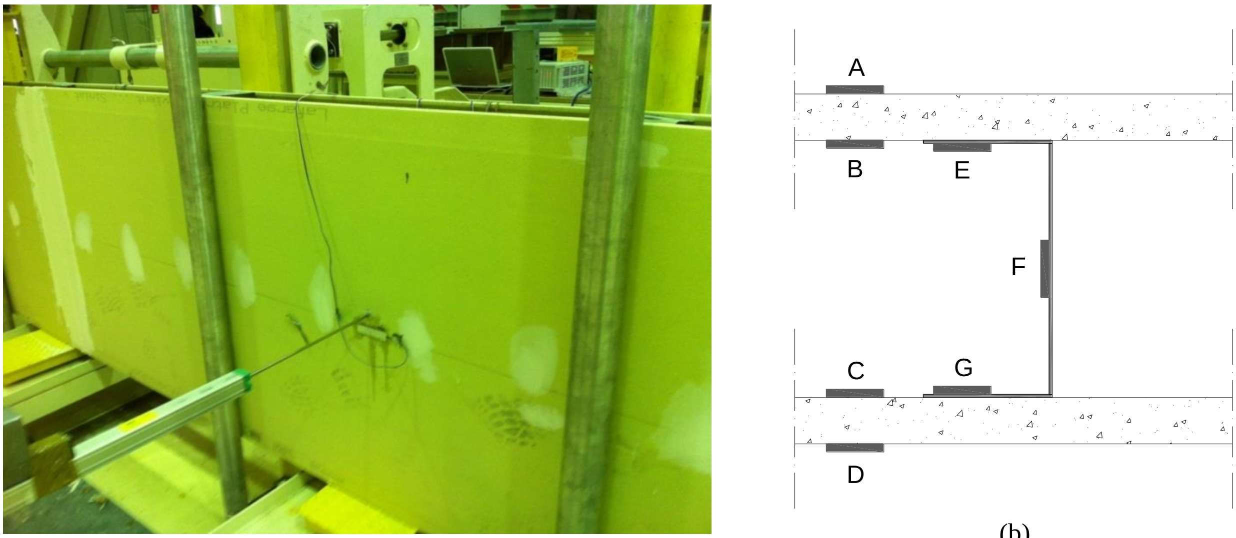

(a) (b)

Figure 7. (a) LVDT used to record the mid-span out-of-plane displacement; (b) strain gauges arrangement in the partition cross-section corresponding to the centroid of the specimen.

3 RESULTS AND DISCUSSION

3.1 Damage description

The different specimens show similar damage typologies. The main damage typologies are:

- cracking of the horizontal joints between adjacent panels (Figure 8a);
- damage of the stud-to-panel screwed connections; it starts from the connections close to the external restraints (Figure 8b) and then affects the ones close to the center of the partition;
- local buckling of either the web or the flange or both the web and the flange of the steel stud, clearly denoted by the waves in the stud (Figure 8c);
- pull out of the boards and/or of the studs from the base or top horizontal guide due to the excessive local plastic deformation in the stud; this damage typology is the typical cause of the collapse of the whole specimen (Figure 8d).

It should be noted that the recorded damage points out that the plasterboards are typically not damaged at the end of the test. Hence, the “weak” part of the tested specimen is either the stud or the horizontal guide or the panel-to-stud screwed connections. Moreover, the recorded damage typologies can be also found in previous experimental studies on plasterboard partition walls, e.g. (Davies et al. 2011; Restrepo and Bersofsky 2011).

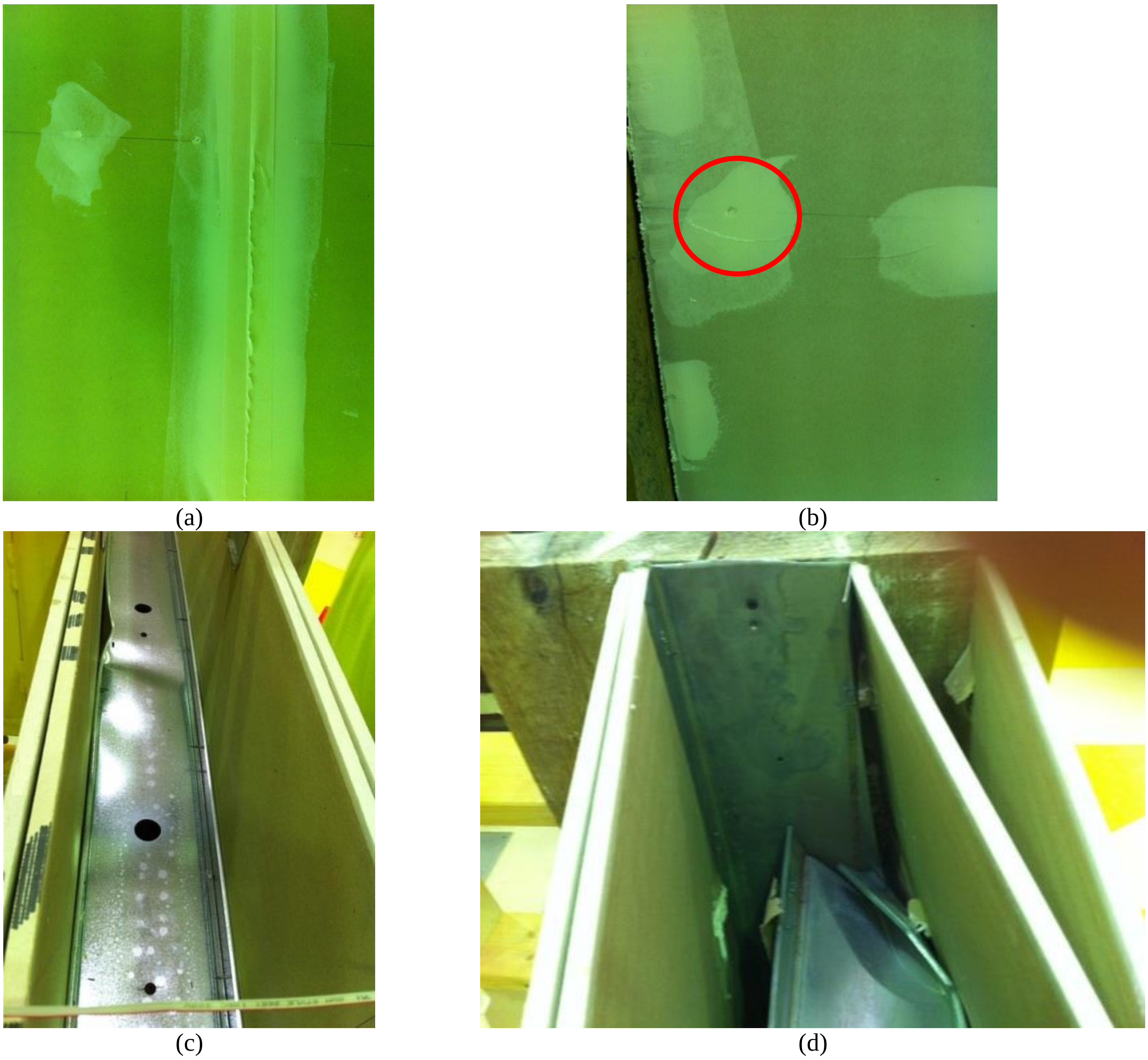

Figure 8. Main recorded damage typologies: (a) paper cracking in the horizontal joints; (b) damage in the panel-to-stud screwed connections; (c) local buckling in the studs; (d) pull out of the stud from the horizontal guide.

3.2 Global behavior: results summary

Recorded forces in the two actuators are similar one another: the static scheme, i.e. the six point bending scheme, is well reproduced during the tests. The total force applied in the out-of-plane direction is plotted versus the centroid out-of-plane displacement in Figure 9 for the four tested specimens. Recorded displacements well agree with the predefined input protocol. A nonlinear behavior of the tested partitions, which occurs after an initial linear trend, is clearly observed. Moreover, their response is unsymmetrical, as highlighted by the different negative and positive strength of the specimens. The occurrence of different damage typologies are also highlighted in the hysteresis loops. The main damage typologies can be summarized in local buckling failure in the studs and joint cracking; the final collapse corresponds for all cases to the pull off of boards and/or of studs from horizontal guides due to local plastic deformation of the guide or failure of the board.

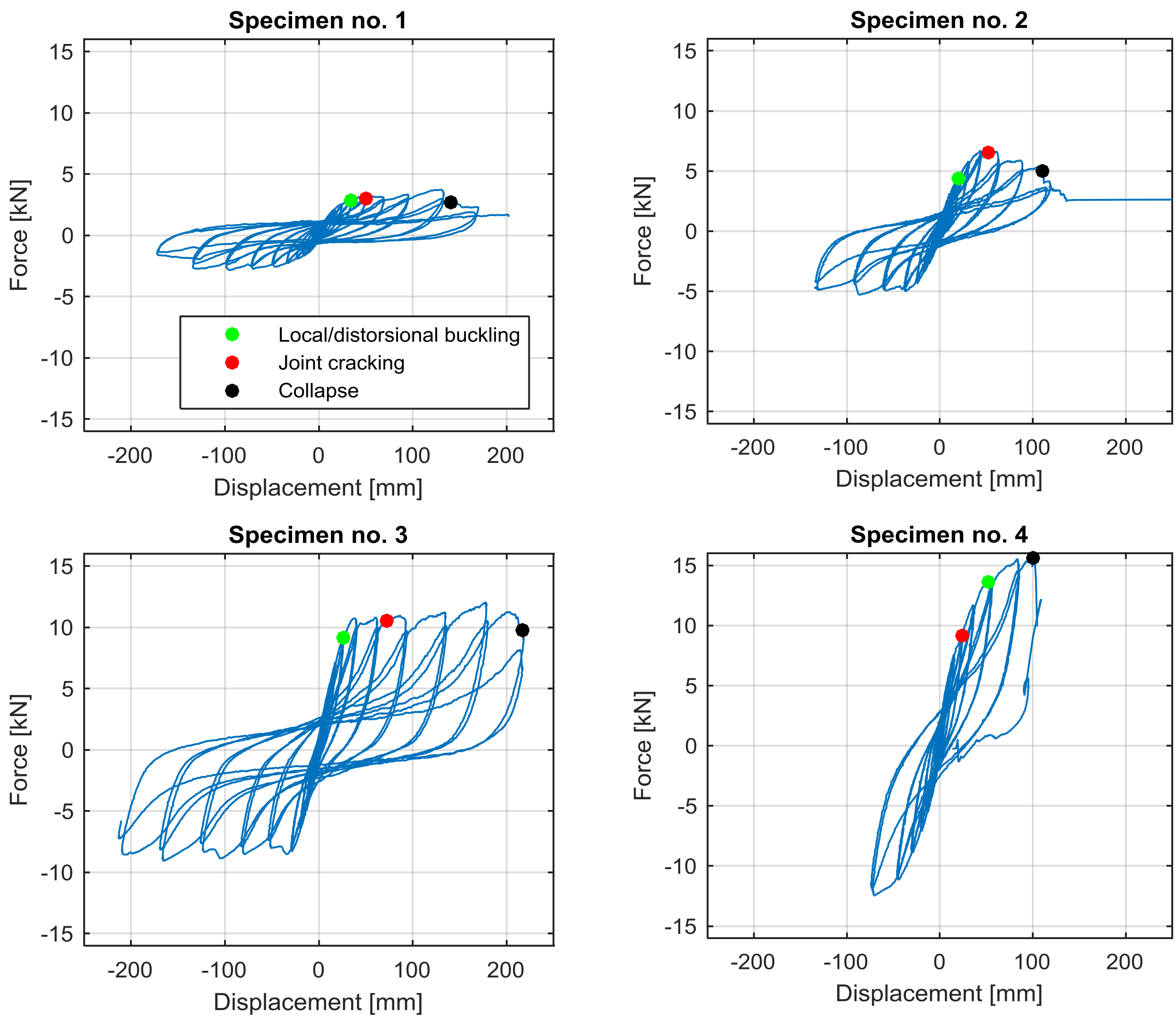

Figure 9. Hysteresis loops for specimens no. 1 - no. 4.

The comparison of the backbone curves (Figure 10a), evaluated as the envelope of the hysteresis loops up to the failure of the specimen, allows evaluating the influence of several parameters:

- specimen no. 3 exhibits a larger strength than specimen no. 2; the introduction of back-to-back studs, which also doubles the amount of screws in the specimen, significantly increases the seismic performance in the out-of-plane direction; indeed, the collapse displacement also increases with the introduction of back-to-back studs;
- specimen no.4 shows the largest strength among the tested specimens, even though specimens no. 3 and no. 2 are characterized by a deeper stud; hence, the contributions to the strength of the specimen of both the thicker boards, i.e. 18 mm thick boards vs 12.5 mm thick boards, and the larger number of studs, i.e. six M100-50 vs four M150-50, are therefore significant; finally, it should be noted that specimen no. 4 is also characterized by a low collapse displacement.

The different specimens exhibit similar secant stiffness trends (Figure 10b), which degrade as the specimens get damaged. The secant stiffness is evaluated both for positive and negative displacements. The following features can be noted observing the trend of the curves:

- specimen no. 4 shows the largest secant stiffness among the tested specimens, even though it is characterized by a 100 mm deep stud; the presence of six studs and the double layer of 18 mm boards per side give a strong contribution to the stiffness of the partition;

- the doubled number of both the studs and, consequently, the screwed connections in specimen no. 3 compared to the specimen no.2 significantly increases the stiffness of the partition in the out-of-plane direction; hence, secant stiffness is significantly influenced by the amount of screwed connections.

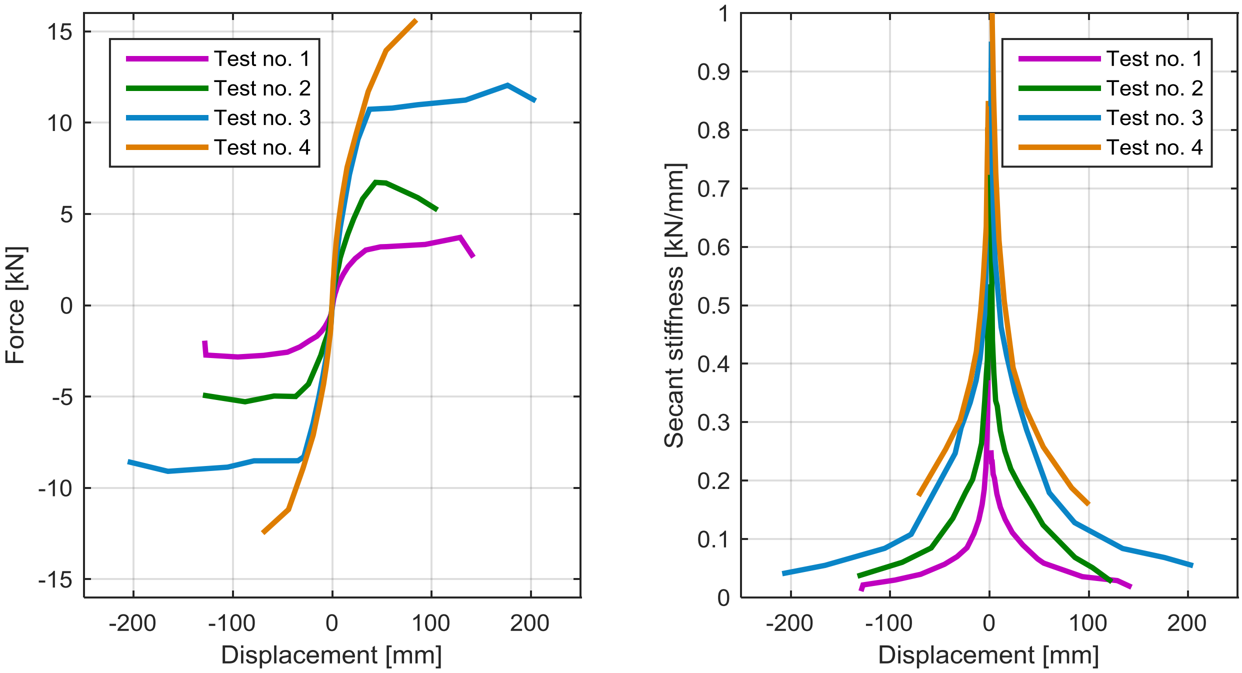

(a) (b)

Figure 10. Comparison among the different tested specimens in terms of (a) backbones curves and (b) secant stiffness.

The hysteresis loops of each single step of the test protocol are isolated in order to underline their shape change during the test. Indeed, in the first steps the force-displacement relationship is almost linear and friction mechanisms are noted; in the last steps a pinching phenomenon is clearly visible in the force-displacement relationships. The pinched behavior is caused by the damage in the screwed connections, whose cyclic behavior is strongly degrading at large displacement levels. The comparison between steps no. 9 and no. 16 for specimen no. 1 (Figure 11) clearly highlights the change in the hysteresis loop shape. The sensitivity of the tested specimen to the selected protocol is therefore demonstrated; it should be underlined that FEMA 461 protocol might be significant different from the seismic action experienced by a partition during a real earthquake.

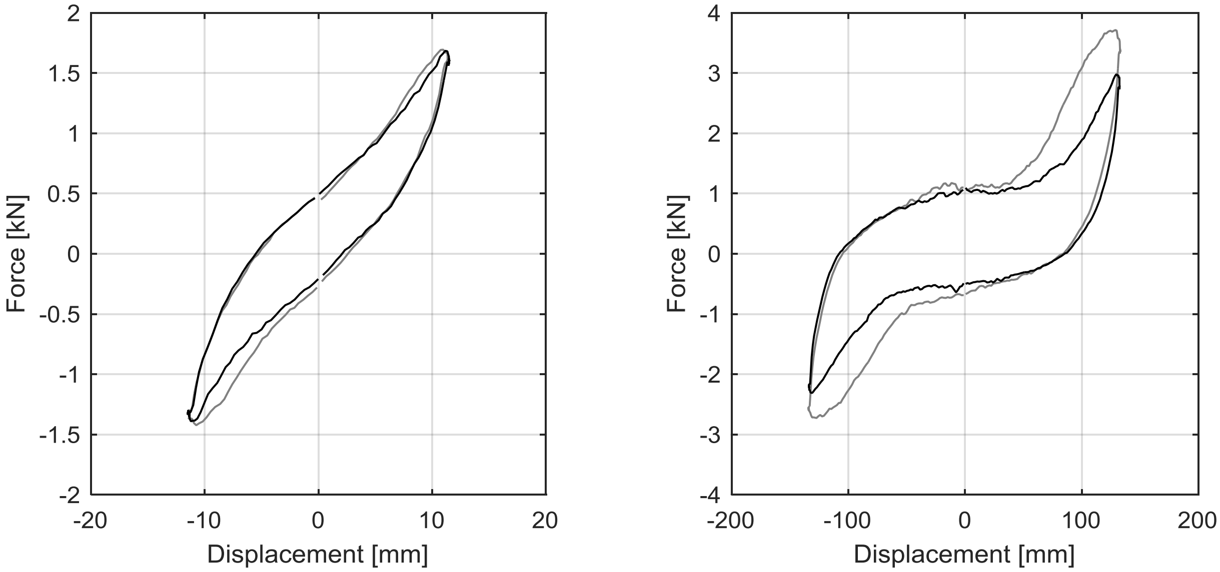

(a) (b)

Figure 11. Force-displacement relationship for (a) step no. 9 and (b) step no. 16 of the defined loading test protocol in specimen no. 1; the first of the two cycles of the step is in gray, whereas the latter cycle is in black.

The dissipated energy in test no. 1 for each negative and positive semicycle of the given protocol is shown in Figure 12. The degrading behavior of the specimen is clearly highlighted. Indeed, the test protocol provides two consecutive cycles at the same displacement (see Section **Error! Reference source not found.**); the energy dissipated in the second cycle of the step is smaller than the energy dissipated in the first cycle of the same step. In particular, the energy reduction among two cycles at the same imposed displacement in specimen no. 1 is 6.2% at step no. 8, where it shows an almost linear trend up to steps no. 16 and 17, where the energy reduction is about 25% (Figure 13a). The same conclusions can be drawn from the dissipated energy trends of the tests no. 2 – no. 4, which show a similar dissipated energy decay among two cycles at the same imposed displacement (Figure 13a).

The energy dissipated in the negative semicycle is similar to the energy dissipated in the preceding positive semicycle for specimen no. 1, even if the negative force is typically smaller than the positive one, i.e. discrepancies up to 12%. Instead, larger discrepancies among positive and negative dissipated energies are found in specimens no.2 to no. 4 (Figure 13b), which confirm the unsymmetrical behavior of the tested partition systems.

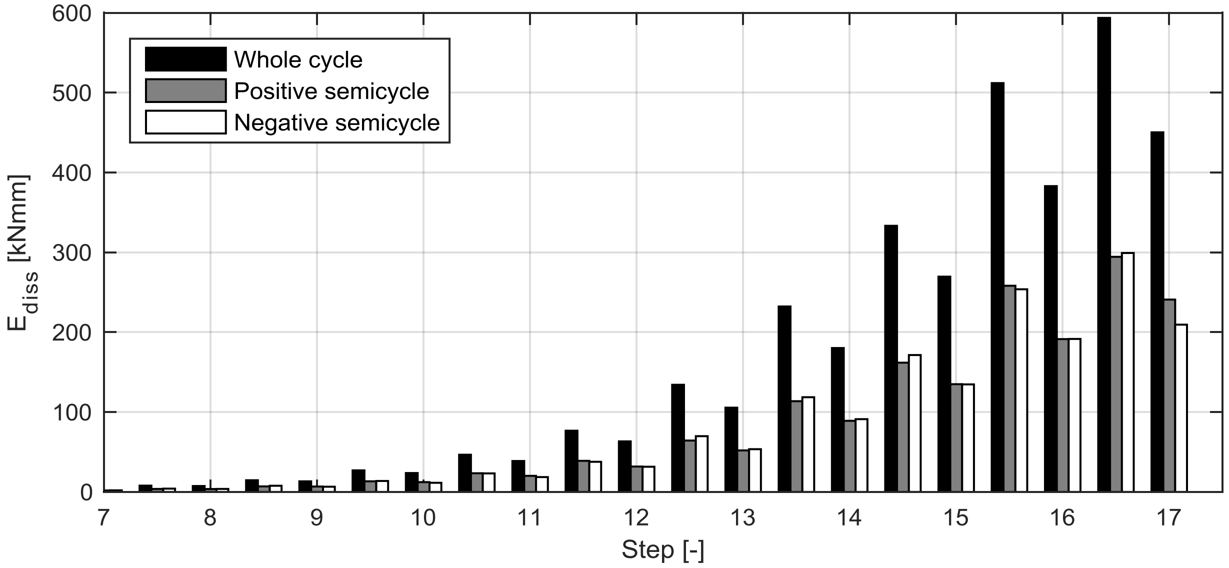

Figure 12. Energy dissipated for each cycle during the test no. 1.

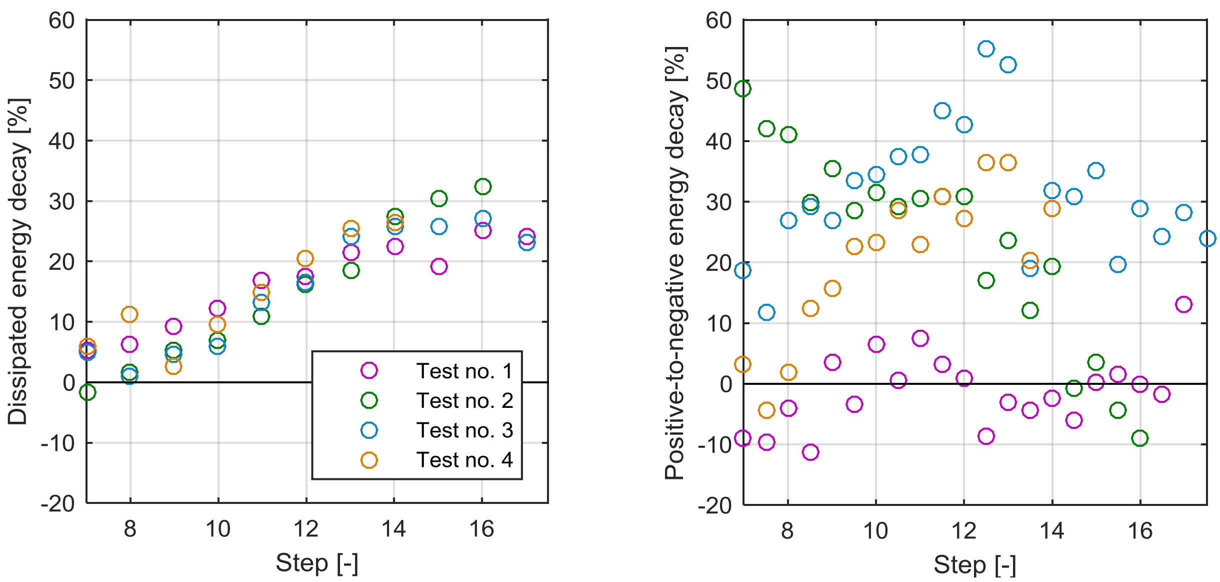

(a) (b)

Figure 13. (a) Dissipated energy decay among two consecutive cycles at the same imposed displacement; (b) dissipated energy decay among positive and negative semicycles.

It should be underlined that the tests were performed in a quasi-static regime. Such a test typology allows evaluating the capacity of the component to compare with the seismic demand. However, a dynamic test might show different modes of failure, besides taking into account the inertia loads and the dynamic behavior of the component. For instance, the delamination of the board from the studs cannot be observed in the performed quasi-static tests, given the adopted test setup; such a mode of failure could be particularly observed in case a bookcase is fixed to the wall.

3.3 Local behavior: contribution of the boards to the resisting bending moment

Section 3.3 shows the contribution of both Siniat boards and screwed connections to both the strength and the stiffness of the partition. In order to highlight their influence on the global behavior of the partition in the out-of-plane direction, the strain gauge recordings are investigated. In Figure 14 the strain recordings on Siniat boards of the specimen no. 1 are shown: the green line shows the deformations recorded on the internal side of the board, whereas the blue line shows the strain recorded on the external side.

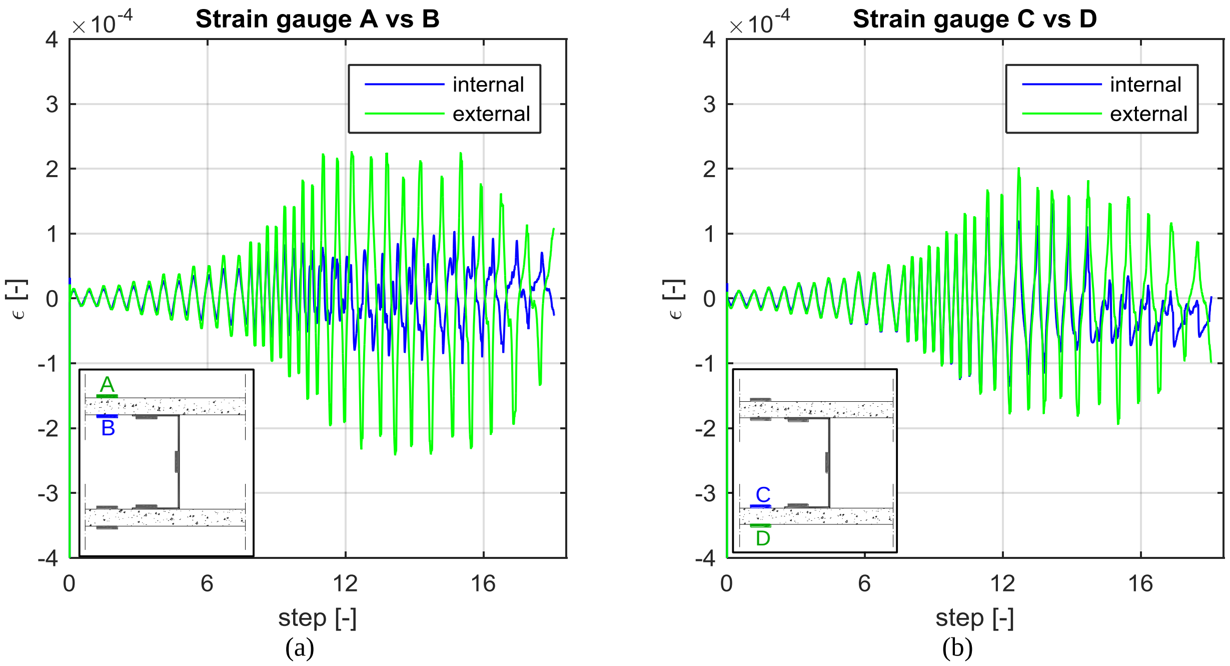

Figure 14. Strain gauge recording in both the sides of the two plasterboards installed in specimen no. 1.

The strains on the internal and external sides are almost coincident during the first cycles of the test; after some cycles they tend to become opposite. This issue suggests that the board-to-stud cross-section behaves as a composite cross-section; two different components, i.e. plasterboards and steel studs, are connected by steel screwed connections in this cross-section.

Initially the stud and the boards behave as a unique cross-section (Figure 15a); as the screwed connections start failing, a relative slip between studs and boards is recorded and the components do not act as a unique cross-section anymore; they tend to act as three different cross-sections in parallel (Figure 15b). This behavior is confirmed by the trend shown in Figure 16, where the strains recorded at the same cross-section location both on the steel stud and on the board are compared for test no. 1. During the first cycles, the steel and plasterboard strains are almost coincident. At large displacement levels, the strain compatibility rule, i.e. plane cross-sections remain plane, is not valid anymore; furthermore, the strains become opposite in sign, as expected according to Figure 15b. Moreover, secant stiffness values attained at the first steps are in line with the stiffness of the composite element, whereas the secant stiffness, evaluated after the connections are fully damaged, is close to the “non-composite” stiffness. As a consequence, the inertia, i.e. the out-of-plane stiffness of the partition, significantly reduces at large displacement levels; this phenomenon might justify the nonlinear stiffness trend exhibited by the partitions (Figure 10b). Hence, the nonlinear behavior exhibited by the different specimens might be attributed both to the local buckling of the studs and, particularly, to the board-to-stud screwed connection damaging. Finally it should be noted that this behavior is also exhibited by the other three tested specimens.

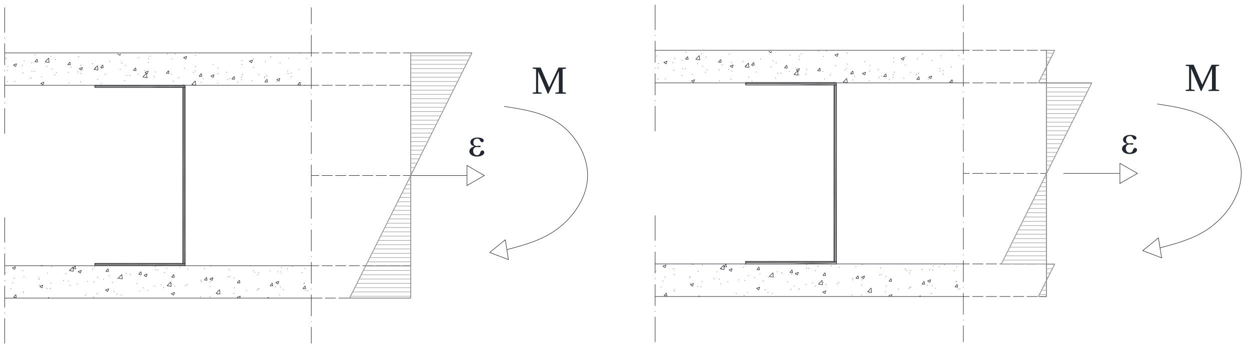

(a) (b)

Figure 15. Plasterboard partition cross-section behavior in terms of recorded strain (a) as a unique composite section and (b) as three different components acting in parallel.

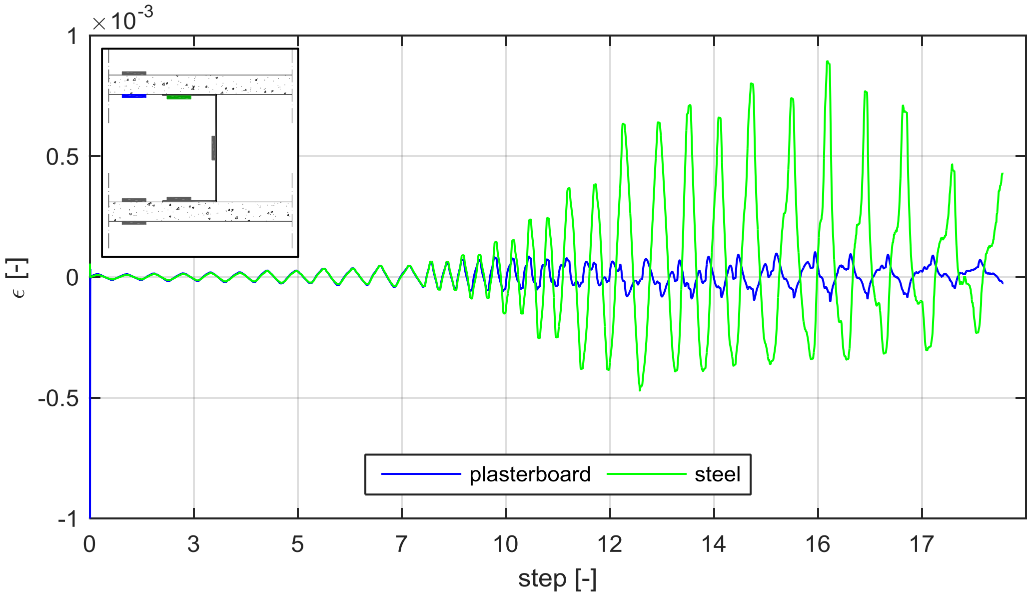

Figure 16. Strain recorded on both steel and plasterboard at the same cross-section position in test no. 1.

3.4 Assessment of the tested partitions: Eurocode vs experiments

According to Eurocode 8 (CEN 2004b), partition walls are nonstructural components, which must be designed according to a seismic demand corresponding to a design seismic intensity level; such intensity level is the same level considered during the design of the primary structure (Petrone et al. 2015b, c). The force-based seismic design of internal partitions is conducted in a straightforward way by comparing the seismic demand on the component with its capacity. Since internal partitions are acceleration-sensitive components in the out-of-plane direction, their assessment is performed in this direction. The assessment of the tested partitions is included in this Section according to Eurocode, which is based on a Load Resistance Factor Design (LFRD). In particular, the seismic demand evaluation is discussed in Section 3.4.1, whereas the assessment of the capacity is included in Section 3.4.2. Finally, Eurocode approach to both the capacity assessment and the global assessment of the tested partitions is compared to the experimental outcomes (Section 3.4.3).

3.4.1 Seismic demand evaluation

According to Section 4.3.5 of Eurocode 8, the seismic demand is determined by applying to the nonstructural element a horizontal force F_a in the out-of-plane direction, which is defined as follows:

$$F_a = \frac{S_a \cdot W_a \cdot \gamma_a}{q_a} \tag{2}$$

where:

- F_a is the horizontal seismic force, acting at the center of mass of the nonstructural element in the considered direction;
- S_a is the seismic coefficient applicable to nonstructural elements, evaluated according to Equation (3);
- W_a is the weight of the element;
- γa is the importance factor of the element, equal to 1 in ordinary conditions;
- q_a is the behavior factor of the element, equal to 2 for internal partitions.

The seismic coefficient S_a may be calculated using the following expression:

$$S_a = \alpha \cdot S \cdot \left[\frac{3 \cdot \left(1 + \frac{z}{H}\right)}{1 + \left(1 - \frac{T_a}{T_1}\right)^2} - 0.5 \right] \tag{3}$$

where:

- α is the ratio between the design peak ground acceleration on stiff soil, a_g, and the acceleration of gravity g;
- S is the soil factor, assumed equal to 1 in this simplified calculation;
- T_a is the fundamental vibration period of the nonstructural element;
- T_1 is the fundamental vibration period of the building in the relevant direction;
- z is the height of the nonstructural element from the foundation or from the top of a rigid basement;
- H is the building height measured from the foundation or from the top of a rigid basement.

The value of the seismic coefficient S_a should not be taken less than $\alpha \cdot S$. For internal partitions, it can be assumed that they are installed at the top story of the structure; moreover, on the safe-side, it is supposed that the fundamental period of the component in the out-of-plane direction is equal to the period of the structure, i.e. T_a/T_1 is set equal to 1. Finally, the maximum bending moment M_{max}, acting in the centroid of the partition, according to a pinned-pinned static scheme is equal to $F_a \cdot h/4$, where h is the interstory height, equal to 5 m for the tested specimens. It should be noted that the assumption on the static scheme is safe-sided compared to a fixed-fixed boundary condition. The maximum axial force acting in the partition is the weight of the partition, whereas the maximum shear force is $F_a/2$. However, as expected, both the axial and the shear forces are negligible compared to the corresponding capacities of the considered partitions. For this reason, the verification is conducted only in terms of bending moment.

3.4.2 Seismic capacity evaluation

The resisting bending moment of the tested partition is evaluated in this paragraph. Unfortunately, formulations that allow taking into account the contribution of the boards to the steel studs are not available in the current building codes, e.g. Eurocode 3 part 1-3 (CEN 2004a). Hence, the resisting bending moment of a plasterboard partition can be evaluated as the capacity of the steel studs included in the considered partition; the presence of the plasterboards allows considering that the seismic demand is equally distributed among the different studs of a partition. According to Eurocode 3 part 1-3 (CEN 2004a), which is related to cold-formed steel elements, the resisting bending moment of a partition can be evaluated as follows:

$$M_{b,Rd} = \chi_{LT} \cdot W_{z,eff} \cdot \frac{f_{yb}}{\gamma_{M1}} \cdot n_{studs} \tag{4}$$

Where χ_{LT} is the reduction factor due to the lateral-torsional buckling, which takes into account several geometrical and mechanical features of the studs, $W_{z,eff}$ is the effective section modulus, f_{yb} is the nominal steel yield strength, γ_{M1} is the partial safety factor and n_{studs} is the total number of studs in the given partition. In the specific case, nominal steel yield strength is set equal to 300 N/mm^2 and partial safety factor is set equal to 1.0, i.e. safety factor is not considered.
It should be noted that the effective section modulus is evaluated according to a reduced “effective” section, where some portions of the cross-section are not considered; this reduction is due to both local and distortional instabilities, as clearly described in Eurocode 3 part 1-3 (CEN 2004a). Since the cross-section of the stud is not symmetric with respect to the neutral axis, the section modulus is taken as the minimum between the positive and negative ones.

3.4.3 Assessment of the tested partitions: Eurocode vs experimental tests

In Figure 17a the resisting bending moments evaluated according to Eurocode 3 are plotted in black for each partition. These values are compared to the strength exhibited by the tested specimens (in white), which is simply evaluated from the maximum force recorded during each test. Such a maximum force is equal to the peak negative force, given the unsymmetrical behavior of the tested specimens (Figure 10a). Eurocode approach shows a strong underestimation of the resistance of the tested specimens. This underestimation suggests that the contribution of Siniat boards to the resisting bending moment, which is neglected in Eurocode 3, is significant. Such a contribution is significant also due to the presence of the screws, which allows the plasterboards to carry a significant amount of bending moment. Indeed, the bending moment absorbed by Siniat plasterboards in the configuration in Figure 15a, where the screwed connections are effective, is much larger than in the configuration in Figure 15b, which is representative of a cross-section without screwed connections.
The performance check of the tested partitions is then assessed by comparing the demand with the capacity in terms of bending moment. In particular, the seismic demand can be evaluated in terms of maximum bending moment according to the assumptions included in Section 3.4.1. In order to generalize the problem, the design peak ground acceleration on stiff soil a_g, required to the seismic demand to equal the seismic capacity (Figure 17a), is evaluated and plotted in Figure 17b. The a_g values evaluated according to Eurocode strength are much lower than a_g typical values in moderate-to-high European seismic zones, which are larger than 0.30 g. In other words, according to Eurocode-based strength assessment, these partitions could not be used in these zones: a larger amount of studs would be needed. Instead, considering the experimental strength, the tested Siniat partitions could be used in almost the whole European territory.
The large discrepancy between the Eurocode and the experimental results obtained on Siniat partitions claims the urgent need to define a formulation that would include the contribution of the plasterboards, through the screws, to the resisting bending moment. However, caution should be taken in generalizing the results since a limited amount of tests was performed, i.e. only one specimen for each partition typology.

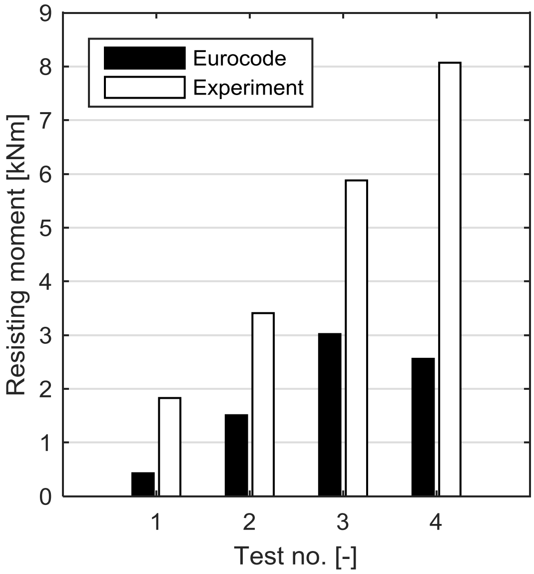

(a)

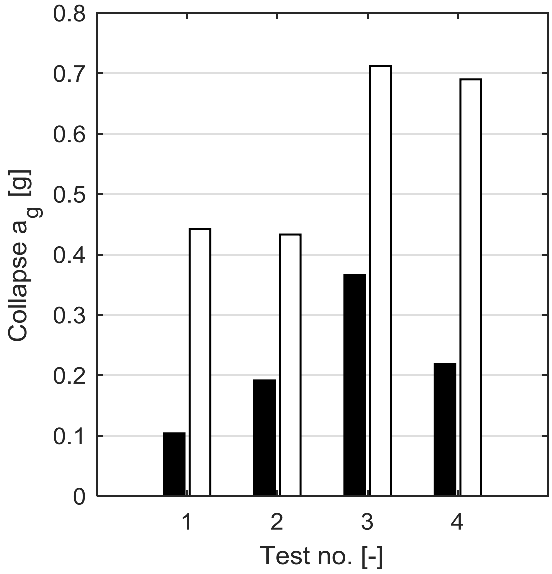

(b)

Figure 17. Comparison between (a) resisting bending moments and (b) collapse ground accelerations evaluated both according to Eurocode and from the experimental tests.

4 CONCLUSIONS

A quasi-static test campaign aimed at the evaluation of the seismic performance of plasterboard internal partitions with steel studs is presented in the paper. The research study deals with the out-of-plane behavior of such a nonstructural component. Four tall, i.e. 5 m high, specimens are selected; they are typical Siniat plasterboard internal partitions installed in Europe. FEMA 461 test protocol is adopted.

The specimens show similar damage typologies at different displacement demand intensities: minor damage states, such as (a) paper cracking in the horizontal joints between adjacent panels, (b) damage of the stud-to-panel screwed connections, (c) local buckling of the steel studs, at low displacement demand; major damage states, such as pulling out of the boards and/or of the studs from the base or top horizontal guide, at larger displacement demand. A significant nonlinear pinched behavior of the tested specimen is observed. The pinched behavior is caused by the damage in the screwed connections, whose cyclic behavior is strongly degrading. The comparison of the backbone curves allows evaluating the influence of some parameters:

- the use of back-to-back studs, which doubles the amount of screws in the specimens, significantly increases the seismic performance in the out-of-plane direction;
- both the stiffness and the strength of the specimens are significantly influenced by the adopted board typology and the amount of screwed connections.

Steel and plasterboard strains at the same cross-section location are equal for low displacement demand, suggesting that the tested components behave as a composite board-stud-board component. The strain compatibility rule, i.e. plane cross-sections remain plane, is then violated as damage in the screwed connections starts occurring. The stud and the two plasterboards behave as three distinct components acting in parallel at that stage. The damage in the screws also causes a reduction of the inertia of the whole cross-section, which might justify the nonlinear stiffness trend exhibited by the tested partitions. Hence, the nonlinear behavior exhibited by the different specimens may be attributed to the board-to-stud screwed connection damage. Finally, the resisting bending moment of the Siniat partitions is evaluated according to Eurocodes and compared to the experimental results. A substantial disagreement between the code and the experimental assessment is shown.

It should be underlined that the tests were performed in a quasi-static regime. Dynamic tests might show different modes of failure which were not exhibited in this research study, due to the nature of the applied load. Future studies will deal with the influence of several parameters that were not considered in this study, such as the environmental conditions and the interaction with sprinkler systems. Moreover, a wide set of partitions, e.g. multiple specimens for each partition typology, is required in order to generalize the results in a design building code.

ACKNOWLEDGEMENTS

This research study has been funded both by Italian Department of Civil Protection in the framework of the national project DPC-ReLUIS 2014 RS8 and by Siniat that also provided the partition systems for the testing program.

The support provided by Eng. Luigi Giannetti in the analysis of the results is gratefully acknowledged. Authors thank Ms. Raffaelina Divano, English language expert, for the paper proofreading.

REFERENCES

ASTM (2015) Standard Test Methods of Conducting Strength Tests of Panels for Building Construction. ASTM E72-15. ASTM, West Conshohocken, PA

Bertero RD, Bertero VV (2002) Performance-based seismic engineering: the need for a reliable conceptual comprehensive approach. Earthq Eng Struct Dyn 31 (3):627-652. doi:10.1002/Eqe.146

CEN (2004a) Eurocode 3: design of steel structures - Part 1-3: Supplementary rules for cold-formed members and sheeting. EN 1993-1-3. Brussels, Belgium

CEN (2004b) Eurocode 8: design of structures for earthquake resistance - Part 1: general rules, seismic actions and rules for buildings. EN 1998-1. Brussels, Belgium.

Davies R, Retamales R, Mosqueda G, Filiatrault A (2011) Experimental Seismic Evaluation, Model Parameterization, and Effects of Cold-Formed Steel-Framed Gypsum Partition Walls on the Seismic Performance of an Essential Facility. Technical Report MCEER-11-0005. University at Buffalo, State University of New York

FEMA 461 (2007) Interim Testing Protocols for Determining the Seismic Performance Characteristics of Structural and Nonstructural Components. Redwood City, California, USA

Ikuta E, Miyano M (2011) Study of Damage to the Human Body Caused by Earthquakes: Development of a Mannequin for Thoracic Compression Experiments and Cyber Mannequin Using the Finite Element Method. In: Spence R, So E, Scawthorn C (eds) Human Casualties in Earthquakes, vol 29. Advances in Natural and Technological Hazards Research. Springer Netherlands, pp 275-289. doi:10.1007/978-90-481-9455-1_19

International Conference of Building Officials (ICBO) (2000) AC 156 Acceptance Criteria for the Seismic Qualification of Nonstructural Components. ICBO Evaluation Service, Inc., Whittier, California, USA

Lee TH, Kato M, Matsumiya T, Suita K, Nakashima M (2007) Seismic performance evaluation of non-structural components: Drywall partitions. Earthq Eng Struct Dyn 36 (3):367-382. doi:10.1002/Eqe.638

Magliulo G, Petrone C, Capozzi V, Maddaloni G, Lopez P, Manfredi G (2014) Seismic performance evaluation of plasterboard partitions via shake table tests. Bull Earthq Eng 12 (4):1657-1677. doi:10.1007/s10518-013-9567-8

Magliulo G, Petrone C, Capozzi V, Maddaloni G, Lopez P, Talamonti R, Manfredi G (2012) Shake Table Tests on Infill Plasterboard Partitions. Open Constr Build Technol J 6 (Suppl 1-M10):155-163. doi:10.2174/1874836801206010155

Peterman K, Schafer B (2014) Sheathed Cold-Formed Steel Studs under Axial and Lateral Load. J Struct Eng 140 (10):04014074. doi:doi:10.1061/(ASCE)ST.1943-541X.0000966

Petrone C, Magliulo G, Lopez P, Manfredi G (2015a) Seismic fragility evaluation of plasterboard partitions via in-plane quasi-static tests. Earthq Eng Struct Dyn (online early). doi:10.1002/eqe.2600

Petrone C, Magliulo G, Manfredi G (2015b) Floor response spectra in RC frame structures designed according to Eurocode 8. Bull Earthq Eng (submitted for publication)

Petrone C, Magliulo G, Manfredi G (2015c) Seismic demand on light acceleration-sensitive nonstructural components in European reinforced concrete buildings. Earthq Eng Struct Dyn (online first). doi:10.1002/eqe.2508

Restrepo JI, Bersofsky AM (2011) Performance characteristics of light gage steel stud partition walls. Thin-Walled Structures 49 (2):317-324. doi:10.1016/j.tws.2010.10.001

Restrepo JI, Lang AF (2011) Study of Loading Protocols in Light-Gauge Stud Partition Walls. Earthq Spectra 27 (4):1169-1185. doi:10.1193/1.3651608

Retamales R, Davies R, Mosqueda G, Filiatrault A (2013) Experimental Seismic Fragility of Cold-Formed Steel Framed Gypsum Partition Walls. J Struct Eng 139 (8):1285-1293. doi:10.1061/(ASCE)ST.1943-541X.0000657

Taghavi S, Miranda E (2003) Response assessment of nonstructural building elements, PEER report 2003/05. College of Engineering, University of California Berkeley, USA

Tasligedik AS, Pampanin S, Palermo A (2012) Damage states and cyclic behaviour of drywalls infilled within rc frames. Bulletin of the New Zealand Society for Earthquake Engineering 45 (2):84-94

Villaverde R (1997) Seismic design of secondary structures: State of the art. J Struct Eng-Asce 123 (8):1011-1019. doi:10.1061/(Asce)0733-9445(1997)123:8(1011)